

Saturation in Liquid/Gas Coalescence

Problem presented by

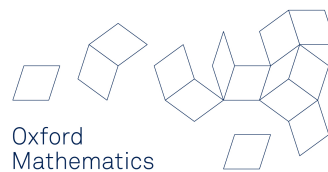
Mark Hurwitz

Pall Corporation



ESGI100 was jointly hosted by
Smith Institute for Industrial Mathematics and System Engineering
University of Oxford

Smith *institute*
for industrial mathematics and system engineering



with additional financial support from
Engineering and Physical Sciences Research Council
European Journal of Applied Mathematics
Oxford Centre for Collaborative Applied Mathematics
Warwick Complexity Centre

Report author

B. Chakrabarti, J. Chakraborty, C. J. Chapman, L. J. Cummings, P. Dondl,
V. Lapin, A. Münch, B. Piette, T. Rafferty, M. Saxton

Executive Summary

The problem was to construct a mathematical model for a liquid/gas coalescer, in order that the model could be analyzed to find combinations of parameters that would minimize the effects of saturation.

The team has developed three complementary models, each with different strengths and weaknesses so that, depending on the information desired, one model may be more useful than another. The three models are:

1. A continuum model giving a macroscopic description of the filter. The governing equations are derived from first-principle considerations of conservation of mass and momentum. Constitutive relations for this model are derived by considering the processes going on in the filter at a microscopic level.
2. A stochastic model based on a Markov Decision Process. Each droplet is modelled as a single entity that can merge or move stochastically. This leads to a Markov simulation of the filter and the computation of average quantities.
3. A Lattice-Boltzmann model. The droplets are modelled to interact with each other and with the filter, using a Boltzmann distribution for their speed. This simulates the hydrodynamic behaviour of the droplet inside the filter.

Version 1.0
May 22, 2014
iv+36 pages

Contributors

- P. Aceves Sanchez (University of Vienna)
- N. Bailey (University of Nottingham)
- M. Bruna (University of Oxford)
- P. Cesana (University of Oxford)
- B. Chakrabarti (Durham University)
- J. Chakraborty (University of Oxford)
- C. J. Chapman (Keele University)
- L. J. Cummings (New Jersey Institute of Technology)
- M. Dallaston (University of Oxford)
- J. Dietz (Pall Corporation)
- P. Dondl (Durham University)
- C. Finn (University of Warwick)
- I. Griffiths (University of Oxford)
- J. Herterich (University of Oxford)
- C. Holloway (University of Birmingham)
- M. Hurwitz (Pall Corporation)
- A. Hutchinson (University of the Witwatersrand)
- R. Kgatle (University of the Witwatersrand)
- D. Khoromskaia (University of Warwick)
- A. Krupp (University of Oxford)
- V. Lapin (University of Leeds)
- N. Letchford (University of Oxford)
- A. Lewis (University of Oxford)
- A. Manhart (University of Vienna)
- M. Moore (University of Oxford)
- A. Münch (University of Oxford)
- H. Ockendon (University of Oxford)
- J. Oliver (University of Oxford)
- D. Paccagnan (Technical University of Denmark)
- A. Patel (Pall Corporation)
- B. Piette (Durham University)
- C. Please (University of Oxford)
- R. Purvis (University of East Anglia)
- T. Rafferty (University of Warwick)
- M. Saxton (University of Oxford)
- D. Stuerzer (Vienna University of Technology)
- Y. Sun (University of Oxford)
- A. Tamsett (University of Warwick)
- J. Uddin (University of Birmingham)
- T. Vo (University of Limerick)
- Y. Wei (University of Oxford)
- M. Zagórowska (Centre for Industrial Applications of Mathematics and Systems Engineering)

Contents

1	Introduction	1
1.1	Background	1
1.2	Objective of the study group	2
1.3	Notation	2
1.4	Typical parameter values	2
1.5	Outline	3
2	Macroscopic Description	4
2.1	General continuum model	4
2.2	Steady-state solutions for simplified models	7
3	Microscopic Description	10
3.1	Capture rate of droplets	11
3.2	Extraction of droplets from fibre to gas	15
3.3	Influence of gravity	15
3.4	Liquid flow rate on fibres	16
3.5	Displacement of large droplets on fibres	16
3.6	Alternative model for droplet coalescence and translation within a filter medium	19
3.7	Fluid flow on fibres	22
3.8	Linking the macroscopic to the microscopic model	26
4	Stochastic Model	27
4.1	Mean-field calculation of droplet size distribution in a thin coalescence filter	27
4.2	Markov model	29
5	Lattice-Boltzmann Computation	31
A	Appendix: Notation for the continuum model	33
	Bibliography	35

1 Introduction

1.1 Background

- (1.1) A liquid/gas coalescer is a non-woven fibrous sheet of filter media, usually formed into a cylinder or pleated cylindrical pack, which is used to remove liquid droplets from gas process streams in situations where the concentration of droplets is low (less than about 1000 parts per million by weight) and the droplet size is small (less than about 10 microns). The flow of gas and droplets is generally radially outward through the pack. The droplets may interact with the fibres, which are randomly oriented and cross each other at many points. Through these interactions, the droplets coalesce to larger sizes and eventually migrate to the outer surface of the pack where they are released at a size large enough to be separated from the gas by gravity. In a typical installation, the axis of the pack is vertical, so that gravity tends to drive a higher concentration of captured droplets at the lower end. This setup is illustrated in figure 1.

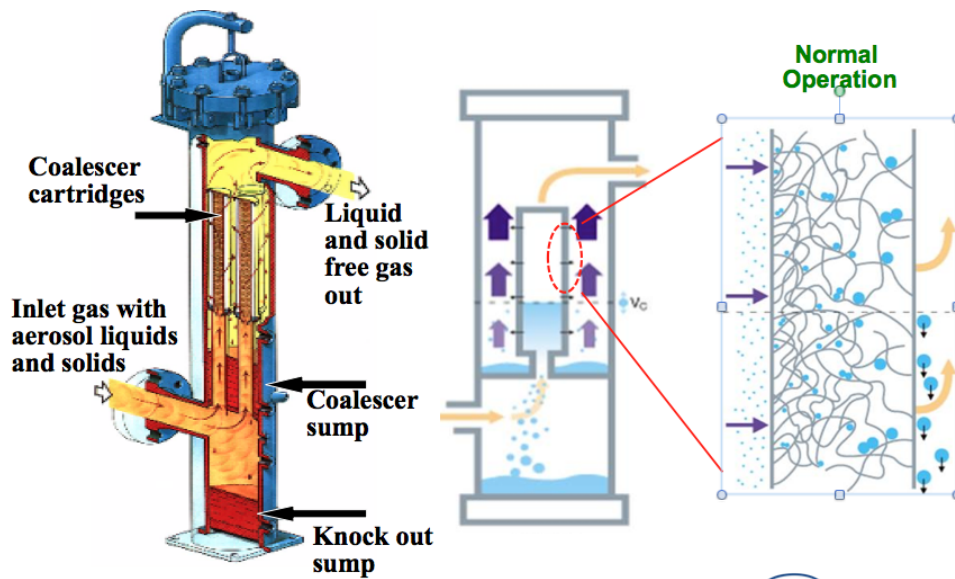


Figure 1: A liquid/gas coalescer. Small liquid droplets enter in the gas stream but then are captured by the fibres inside the filter. The droplets then coalesce on the fibres so that the droplets emerging from the filter are sufficiently large to be removed by gravity. *Image provided by Pall Corporation.*

- (1.2) If the concentration of droplets within the sheet becomes too large, the gas flow will exert too large a force, the coalescing process will be disrupted, and random-sized droplets will be released, many as small as the original droplets in the feed stream. This condition is called saturation. A cross-section of a saturated filter is shown in figure 2.

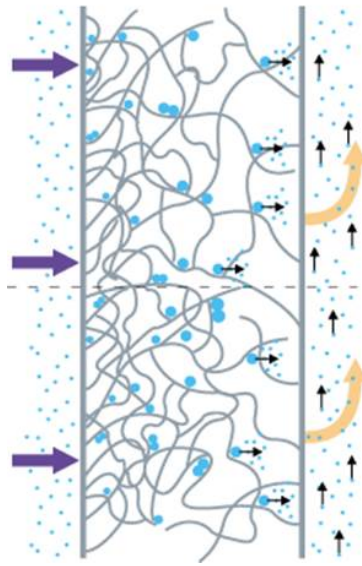


Figure 2: Cross-section of a saturated filter. The liquid droplets released from the filter are too small and so are carried off in the gas stream rather than being removed by gravity. *Image provided by Pall Corporation.*

1.2 Objective of the study group

- (1.3) Pall Corporation is interested in understanding the conditions under which saturation is likely to occur, and possibly finding optimal combinations of gas velocity, fibre diameter, fibre spacing and fibre surface energy to minimize its effects. The study group team therefore constructed mathematical models for the processes going on in the filter, ultimately developing three different possible models. In principle, it is possible to analyze these models in order to find combinations of parameters that will minimize the effects of saturation.

1.3 Notation

- (1.4) The notation relating to the continuum model, used throughout §§2–3 of the report, is shown in tables 3–5 in the Appendix for reference. The notation used in the discrete models in §§4–5 is defined therein.

1.4 Typical parameter values

- (1.5) Table 1 shows typical values of the physical parameters involved in the models. The upper section of the table gives parameter values, provided by the representatives of Pall Corporation, for a typical filter. Typically, the liquid being filtered out of the natural gas stream is hexane, and the material from which the fibres are made is Teflon (PTFE); typical parameter values

for this liquid and fibre material, obtained from the internet, are shown in the lower section of the table.

Symbol	Parameter	Value
H	Column height	$\approx 1\text{m}$
P_0	Inlet pressure	$500 - 600\text{PSI} \approx 4\text{M Pa}$
ΔP	Pressure drop across filter	$0.01P_0 \approx 40\text{kPa}$
d_d	Inlet droplet diameter	$0.1 - 10\mu\text{m}$
α_{id}	Inlet liquid fraction	$1 - 10\text{ppm Vol}$
v_G	Gas face velocity at the inlet	$0.05 - 0.15\text{m/s}$
l_M	Media thickness	$5\text{mm} \pm 2.5\text{mm}$
T	Temperature inside the filter	$100^\circ\text{F} \approx 38^\circ\text{C}$
d_f	Fibre diameter	$2 - 5\mu\text{m}$
l_f	Typical distance between fibres	$10\mu\text{m}$
ϕ	Filter void fraction	$80 - 90\%$
γ_{LG}	Hexane Surface Tension at 40 deg	0.017N/m
-	Teflon (PTFE) Surface Tension	0.02N/m
ρ_G	Natural Gas density (at 900PSI)	250kg m^{-3}
μ_G	Natural Gas Viscosity	10^{-5}Pa s
ρ_L	Hexane Density	655kg m^{-3}
μ_L	Hexane Viscosity	$2.94 \times 10^{-4}\text{Pa s}$
-	Hexane-Teflon contact angle	12°

Table 1: Typical values of physical parameters.

1.5 Outline

- (1.6) In §2.1, we derive a continuum model which gives a macroscopic description of the filter. The equations are derived via standard considerations of conservation of mass and momentum. To close this macroscopic model, it is necessary to prescribe constitutive relations for the deposition rate of liquid from the gas stream onto the fibres and for the frictional force (per unit volume) acting on the liquid attached to the fibres. In §2.2, we construct explicit solutions for some simplified versions of this model.
- (1.7) In §3, we consider the processes going on in the filter at a microscopic level. We begin by considering the mass transfer of liquid between the gas and the fibres (§§3.1–3.2). We then briefly consider what role gravity plays at a microscopic level (§3.3). Next we look at how to model the flow of the liquid attached to the fibres through the fibre network (§§3.4–3.7). Finally, we consider how to use this microscopic information to obtain expressions for the constitutive relations needed to close the macroscopic continuum model (§3.8).

- (1.8) In §4 and §5, we derive two discrete models. The first is a stochastic model, with the droplets on a grid of sites, which uses a Markov Decision Process to model movement of droplets through the filter; the second is a lattice-Boltzmann model, which simulates the hydrodynamic behaviour of a droplet inside the filter.

2 Macroscopic Description

2.1 General continuum model

(2.1) *Phase fractions*

A coalescence filter may be modelled as network of fibres through which there flows a stream of fluid comprising both gas and liquid. The fluid occupies a proportion ϕ of the total volume of the filter, and the fibres occupy the remaining proportion $1 - \phi$. The parameter ϕ is the void fraction; in a coalescence filter its value is high, typically in the range 0.8 to 0.9, which is about twice the value in, for example, a random packing of spherical particles. The void fraction is modelled as a constant.

- (2.2) The liquid in the incoming stream of gas is in the form of small suspended droplets, convected with the gas flow. The purpose of the filter is to transfer these droplets to the fibres, either to create large droplets of liquid attached to individual fibres or to their crossing-points, or to create layers of liquid which coat the fibres. In order to model the macroscopic state of the filter, we introduce three further fractions to specify the proportion of fluid volume in the phases (i) gas, (ii) liquid in the gas flow (i.e. small liquid droplets), and (iii) liquid attached to the fibres. These fractions are α_G , α_{LG} , and α_{LM} , expressed as proportions of the total volume of fluid, i.e. excluding the fibres, and so

$$\alpha_G + \alpha_{LG} + \alpha_{LM} = 1. \quad (1)$$

- (2.3) Here the subscript ‘M’ is a generic symbol for the medium (or media) comprising the filter, and so the subscript ‘LM’ denotes the liquid attached to the fibres.

- (2.4) Since volume integrals are performed over the total volume, including the fibres, it is convenient to bear in mind the simple identity

$$\phi\alpha_G + \phi\alpha_{LG} + \phi\alpha_{LM} + (1 - \phi) = 1, \quad (2)$$

in which the successive terms are the proportions of the total volume occupied by the gas, liquid in gas, liquid on fibres, and fibres. The identity expresses the fact that all of space is occupied.

- (2.5) The fractions α_G , α_{LG} , and α_{LM} are functions of position and time, *i.e.* are state variables. One of the main purposes of the macroscopic analysis is

to determine these functions as part of the solution of a complete set of equations of motion, including initial and boundary conditions. The three functions may be regarded as specifying the operating condition of the filter as function of time. In particular, they determine where and when the filter is saturated. In a parametric study, one might, for example, gradually increase the flow rate, to determine where the model predicts that the filter first becomes saturated, and to determine the flow rate at which this occurs.

(2.6) *Conservation of mass*

Although the gas and the suspended liquid droplets form a two-phase flow, they are modelled as having a common velocity \mathbf{u}_G . Thus the Darcy velocity, i.e. combined macroscopic volume flow per unit area per unit time, is $(\alpha_G + \alpha_{LG})\phi\mathbf{u}_G$. This appears to be the simplest notation for our purposes, given that much of the investigation involves microscopic modelling in which the fundamental velocity is \mathbf{u}_G ; but it means that Darcy's law has an extra factor $(\alpha_G + \alpha_{LG})\phi$ compared with its usual expression. Hence some care is necessary when combining our equations with those obtained elsewhere, especially those in which the focus is exclusively on macroscopic behaviour; a quantity denoted \mathbf{u}_G would then almost certainly have a different definition from ours.

(2.7) The gas passes through the filter without mass transfer to any other phase, but the liquid droplets are transferred to the fibres at a deposition rate f_d , defined as the deposited mass of liquid per total volume (including fibres) per unit time. The liquid on the fibres has velocity \mathbf{u}_L . These are macroscopic state variables, i.e. are functions of position and time representing spatial averages over microscopic quantities, as used in the general theory of composite media. Simple control volume analysis, followed by use of the divergence theorem, gives the conservation of mass equation for each phase as

$$\frac{\partial}{\partial t}(\rho_G\alpha_G\phi) + \nabla \cdot (\rho_G\alpha_G\phi\mathbf{u}_G) = 0, \quad (3)$$

$$\frac{\partial}{\partial t}(\rho_L\alpha_{LG}\phi) + \nabla \cdot (\rho_L\alpha_{LG}\phi\mathbf{u}_G) = -f_d, \quad (4)$$

$$\frac{\partial}{\partial t}(\rho_L\alpha_{LM}\phi) + \nabla \cdot (\rho_L\alpha_{LM}\phi\mathbf{u}_L) = f_d. \quad (5)$$

(2.8) *Conservation of momentum*

In deriving the macroscopic momentum equations, it is convenient to regard the gas and suspended liquid droplets as forming a single phase. The forces acting on this combined phase are the pressure gradient, gravity (which may be negligible), and a frictional force given by Darcy's law. Hence the

momentum equation for this phase, expressed in conservation form, is

$$\begin{aligned} \frac{\partial}{\partial t} \{(\rho_L \alpha_{LG} + \rho_G \alpha_G) \phi \mathbf{u}_G\} + \nabla \cdot \{(\rho_L \alpha_{LG} + \rho_G \alpha_G) \phi \mathbf{u}_G \otimes \mathbf{u}_G\} \\ = -\nabla p + (\rho_L \alpha_{LG} + \rho_G \alpha_G) \phi \mathbf{g} - \frac{\mu_G}{k_G} (\alpha_{LG} + \alpha_G) \phi \mathbf{u}_G. \end{aligned} \quad (6)$$

(2.9) Here p is the pressure and \mathbf{g} is the acceleration due to gravity. The terms μ_G and k_G are the dynamic viscosity and the permeability of the combined phase. Subtracting a multiple of the conservation of mass equation gives the momentum equation in its non-conservation form as

$$\begin{aligned} (\rho_L \alpha_{LG} + \rho_G \alpha_G) \phi \left(\frac{\partial \mathbf{u}_G}{\partial t} + \mathbf{u}_G \cdot \nabla \mathbf{u}_G \right) \\ = -\nabla p + (\rho_L \alpha_{LG} + \rho_G \alpha_G) \phi \mathbf{g} - \frac{\mu_G}{k_G} (\alpha_{LG} + \alpha_G) \phi \mathbf{u}_G + f_d \mathbf{u}_G. \end{aligned} \quad (7)$$

(2.10) The last term represents the ‘deposition of momentum’ associated with the mass deposition f_d ; this momentum transfer is implicit in the conservation form of the momentum equation.

(2.11) In the momentum equation for the liquid attached to the fibres, Darcy’s law for the frictional force does not apply. Instead, detailed microscopic modelling is required, as given elsewhere in this report, and here we simply represent the resulting force by the quantity \mathbf{F}_{LM} , defined as the frictional force per total volume (including fibres) acting on the liquid attached to the fibres. Hence the momentum equation for this liquid phase, expressed in conservation form, is

$$\frac{\partial}{\partial t} (\rho_L \alpha_{LM} \phi \mathbf{u}_L) + \nabla \cdot (\rho_L \alpha_{LM} \phi \mathbf{u}_L \otimes \mathbf{u}_L) = -\nabla p + \rho_L \alpha_{LM} \phi \mathbf{g} + \mathbf{F}_{LM}. \quad (8)$$

(2.12) Subtracting a multiple of the conservation of mass equation gives the non-conservation form

$$\rho_L \alpha_{LM} \phi \left(\frac{\partial \mathbf{u}_L}{\partial t} + \mathbf{u}_L \cdot \nabla \mathbf{u}_L \right) = -\nabla p + \rho_L \alpha_{LM} \phi \mathbf{g} + \mathbf{F}_{LM} - f_d \mathbf{u}_L. \quad (9)$$

(2.13) *Constitutive relations*

The dependence of f_d and \mathbf{F}_{LM} on other variables may be regarded as constitutive relations for the filter. Let us use a vector $\boldsymbol{\lambda}_{LM}$ to represent the relevant microscopic variables in a particular model; these might include the average size of the droplets on the liquid attached to the fibres, together with a variable for the range of sizes. Then typical constitutive relations might take the form

$$f_d = f_d(\alpha_{LG}, \alpha_{LM}, \mathbf{u}_G, \boldsymbol{\lambda}_{LM}) \quad (10)$$

and

$$\mathbf{F}_{LM} = \mathbf{F}_{LM}(\alpha_{LM}, \mathbf{u}_G, \mathbf{u}_L, \boldsymbol{\lambda}_{LM}). \quad (11)$$

(2.14) Such constitutive relations are ‘link functions’ which unite the microscopic and macroscopic aspect of the problem. The operational requirements of a filter are macroscopic, but they determine what level of detail is required in the microscopic modelling.

(2.15) *The complete system of equations*

If the microscopic variables and the constitutive relations are regarded as given, there are ten dependent variables in the above equations: these are the three phase fractions α_G , α_{LG} , and α_{LM} ; the three velocity components of \mathbf{u}_G and the three of \mathbf{u}_L ; and the pressure p . We have derived ten independent relations between them, namely three conservation of mass equations; two vector momentum equations giving a total of six component equations; and an equation stating that the sum of the phase fractions is 1. All other quantities are parameters with assumed values; these include the densities ρ_G and ρ_L and the void fraction ϕ .

(2.16) Thus we have obtained the correct number of equations for our set of dependent variables, and in principle these equations may be solved if suitable initial and boundary values are specified. The complete system of equations may be taken to be (1), (3)–(6), and (8). If a non-conservation form of the momentum equations is preferred, (6) and (8) may be replaced by (7) and (9).

(2.17) For any but the simplest microscopic model, it will not usually be accurate to take the microscopic variables as given. The following procedure may then be adopted. If it is decided to model n microscopic variables, then n further equations relating these variables are derived, using the full details of the microscopic model, and these equations are included with those we have obtained already. This gives $n + 10$ equations in $n + 10$ variables, i.e. provides a complete system. The n microscopic variables appear as arguments in f_d and \mathbf{F}_{LM} . In practice, one would take n to be as small as possible, consistent with the purposes at hand. A hierarchy of models could be obtained, by successively increasing the value of n . Such a hierarchy could be a powerful tool in practice.

2.2 Steady-state solutions for simplified models

(2.18) *Simplifications*

Motivated by the goal of obtaining an explicit steady-state solution to the continuum model, we proceed here with some physically intuitive simplifications. First, we assume that the deposition rate f_d is solely dependent on the fraction of liquid in the gas; for mathematical simplicity, we choose the linear dependence

$$f_d = \beta \alpha_{LG}, \quad (12)$$

where β is a constant of proportionality. We further assume that the momentum equations for the liquid and gas, (7) and (9), can be replaced by Darcy's Law, so that they become

$$\mathbf{u}_G = -\frac{k_G}{\mu_G}(\nabla p - \rho_G \mathbf{g}), \quad (13)$$

$$\mathbf{u}_L = -\frac{k_{LM}}{\mu_L}(\nabla p - \rho_L \mathbf{g}). \quad (14)$$

(2.19) However, Darcy's Law with a constant permeability is not an appropriate model for the liquid flow on fibres. We therefore prescribe the following constitutive relation for the permeability of the filter by the liquid on the fibres, k_{LM} , based on an experimental fit [1]:

$$k_{LM} = k_{LM0} \alpha_{LM}^3. \quad (15)$$

Here k_{LM0} is a reference value for k_{LM} .

(2.20) The momentum equations decouple from the model, and we are left with four scalar equations for the steady-state volume fractions α_G , α_{LG} and α_{LM} , and the pressure p . These equations are

$$\alpha_G + \alpha_{LG} + \alpha_{LM} = 1, \quad (16)$$

$$\nabla \cdot \left(\alpha_G \frac{k_G}{\mu_G} (\nabla p - \rho_G \mathbf{g}) \right) = 0, \quad (17)$$

$$\nabla \cdot \left(\alpha_{LG} \frac{k_G}{\mu_G} (\nabla p - \rho_G \mathbf{g}) \right) = \frac{\beta \alpha_{LG}}{\phi \rho_L}, \quad (18)$$

$$\nabla \cdot \left(\alpha_{LM}^4 \frac{k_{LM0}}{\mu_L} (\nabla p - \rho_L \mathbf{g}) \right) = -\frac{\beta \alpha_{LG}}{\phi \rho_L}. \quad (19)$$

(2.21) *One-dimensional model*

To obtain a qualitative estimate of the volume fractions and flow variables, we also neglect the influence of gravity—thus effectively making our model one-dimensional. In this case, equations (16)–(19) become

$$\alpha_G + \alpha_{LG} + \alpha_{LM} = 1, \quad (20)$$

$$\frac{\partial}{\partial x} \left(\alpha_G \frac{k_G}{\mu_G} \frac{\partial p}{\partial x} \right) = 0, \quad (21)$$

$$\frac{\partial}{\partial x} \left(\alpha_{LG} \frac{k_G}{\mu_G} \frac{\partial p}{\partial x} \right) = \frac{\beta \alpha_{LG}}{\phi \rho_L}, \quad (22)$$

$$\frac{\partial}{\partial x} \left(\alpha_{LM}^4 \frac{k_{LM0}}{\mu_L} \frac{\partial p}{\partial x} \right) = -\frac{\beta \alpha_{LG}}{\phi \rho_L}. \quad (23)$$

(2.22) We non-dimensionalize the system of equations using the scheme

$$p = (\Delta P) \tilde{p} + p_0, \quad x = W \tilde{x}, \quad (24)$$

where tildes indicate dimensionless variables, ΔP is the pressure difference between the inlet and the outlet sides of the filter, and W is the width of the filter. To make all dependent variables of comparable size, we use the additional scalings

$$\alpha_{\text{LG}} = \alpha_{\text{LG}0} \tilde{\alpha}_{\text{LG}}, \quad \alpha_{\text{LM}} = \alpha_{\text{LM}0} \tilde{\alpha}_{\text{LM}}, \quad \alpha_{\text{G}} = \tilde{\alpha}_{\text{G}}, \quad (25)$$

where $\alpha_{\text{LG}0}$ and $\alpha_{\text{LM}0}$ are reference values for the relevant volume fractions. This gives the dimensionless equations

$$\frac{\partial}{\partial \tilde{x}} \left(\tilde{\alpha}_{\text{G}} \frac{\partial \tilde{p}}{\partial \tilde{x}} \right) = 0, \quad (26)$$

$$\frac{\partial}{\partial \tilde{x}} \left(\tilde{\alpha}_{\text{LG}} \frac{\partial \tilde{p}}{\partial \tilde{x}} \right) = A \tilde{\alpha}_{\text{LG}}, \quad (27)$$

$$\frac{\partial}{\partial \tilde{x}} \left(\tilde{\alpha}_{\text{LM}}^4 \frac{\partial \tilde{p}}{\partial \tilde{x}} \right) = -B \tilde{\alpha}_{\text{LG}}, \quad (28)$$

where

$$A = \frac{\beta W^2 \mu_{\text{G}}}{\phi \rho_{\text{L}} (\Delta P) k_{\text{G}}} \quad \text{and} \quad B = \frac{\beta W^2 \mu_{\text{L}} \alpha_{\text{LG}0}}{\phi \rho_{\text{G}} (\Delta P) k_{\text{LM}0} \alpha_{\text{LM}0}^4}.$$

(2.23) We also prescribe the boundary conditions

$$\tilde{p}(0) = 1, \quad \tilde{p}(1) = 0, \quad (29)$$

$$\tilde{\alpha}_{\text{LG}}(0) = 1, \quad (30)$$

$$\tilde{\alpha}_{\text{LM}}(0) = 0. \quad (31)$$

(2.24) We now assume that $\tilde{\alpha}_{\text{G}}$ is approximately constant. From this we immediately obtain the linear relation

$$\tilde{p} = 1 - \tilde{x}, \quad (32)$$

and hence obtain analytical solutions for the volume fractions $\tilde{\alpha}_{\text{LG}}$ and $\tilde{\alpha}_{\text{LM}}$ in the form

$$\tilde{\alpha}_{\text{LG}} = \exp(-A\tilde{x}), \quad (33)$$

$$\tilde{\alpha}_{\text{LM}} = \left[\frac{B}{A} (1 - \exp(-A\tilde{x})) \right]^{1/4}. \quad (34)$$

(2.25) These solutions are plotted in figure 3.

(2.26) *Two-dimensional model, including the effects of gravity*

We now extend our simplified model to two dimensions and include the effects of gravity. The relevant dimensional equations are (16)–(19), but with $\nabla = (\partial_x, \partial_y)$. We non-dimensionalize as in the one-dimensional case,

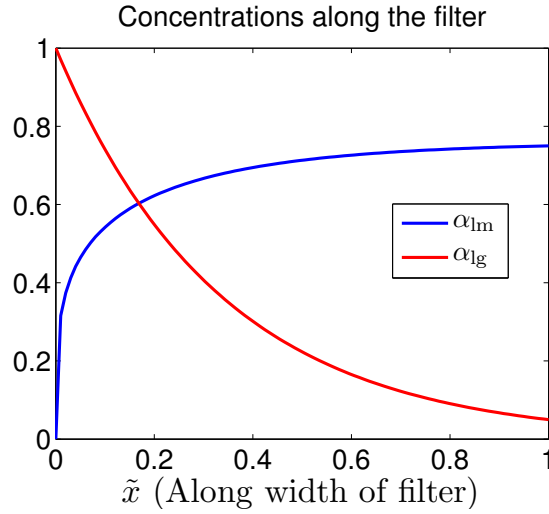


Figure 3: Plots of the partial volume fractions of the liquid in the gas and the liquid on the media in a steady-state condition of the coalescence filter.

with the additional scaling $y = H\tilde{y}$, where H is the height of the filter. This gives

$$\frac{\partial}{\partial \tilde{x}} \left(\tilde{\alpha}_G \frac{\partial \tilde{p}}{\partial \tilde{x}} \right) + \varepsilon^2 \frac{\partial}{\partial \tilde{y}} \left(\tilde{\alpha}_G \frac{\partial \tilde{p}}{\partial \tilde{y}} \right) = 0, \quad (35)$$

$$\frac{\partial}{\partial \tilde{x}} \left(\tilde{\alpha}_{LG} \frac{\partial \tilde{p}}{\partial \tilde{x}} \right) + \varepsilon^2 \frac{\partial}{\partial \tilde{y}} \left(\tilde{\alpha}_{LG} \frac{\partial \tilde{p}}{\partial \tilde{y}} \right) = A\tilde{\alpha}_{LG}, \quad (36)$$

$$\left[\frac{\partial}{\partial \tilde{x}} \left(\tilde{\alpha}_{LM}^4 \frac{\partial \tilde{p}}{\partial \tilde{x}} \right) + \varepsilon^2 \frac{\partial}{\partial \tilde{y}} \left(\tilde{\alpha}_{LM}^4 \frac{\partial \tilde{p}}{\partial \tilde{y}} \right) \right] - \varepsilon E \frac{\partial}{\partial \tilde{y}} (\tilde{\alpha}_{LM}) = -B\tilde{\alpha}_{LG}, \quad (37)$$

with dimensionless parameters

$$E = \frac{\rho_L g W}{\Delta P}, \quad \varepsilon = \frac{W}{H}.$$

(2.27) Here g is the acceleration due to gravity. The parameter E is the ratio of the gravitational force on the liquid to the force due to the pressure difference across the width of the filter, and ε is the ratio of the width of the filter to its height.

(2.28) Since $\varepsilon \ll 1$, it can be easily seen from (35)–(37) that, unless E is of order $1/\varepsilon$ or larger, the leading-order equations are the same as those obtained for the 1-D problem having the same boundary conditions (with no dependence on \tilde{y}). In other words, gravity is not important at leading order.

3 Microscopic Description

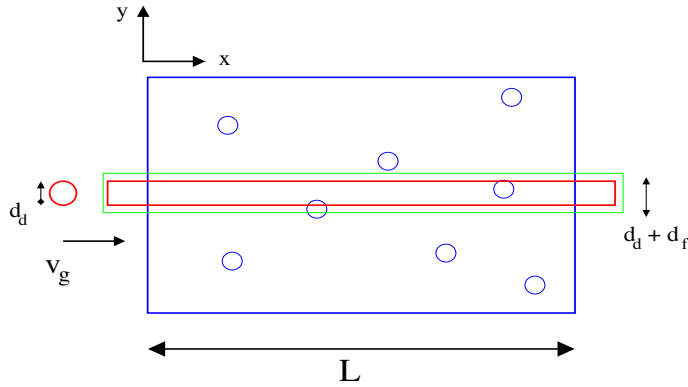


Figure 4: Schematic figure showing collisions of droplets with fibres. The fibres, indicated by blue circles, are perpendicular to the plane of view, while a droplet, indicated by a red circle, sweeps a cylindrical area perpendicular to the fibres. The gas flows from left to right.

3.1 Capture rate of droplets

(3.1) In this section we estimate the capture rate of droplets by the fibres. We start by considering only simple collisions between droplets and fibres, assuming that they move on straight lines. We then consider how our results are modified when we not only assume that small droplets follow the gas flow, but also take into account the effect of diffusion.

(3.2) First of all, we assume that all the fibres are of diameter d_f (radius r_f), and are straight and parallel to each other. We then consider droplets of diameter d_d (radius r_d) moving on straight lines at average speed u_G (equal to the speed of the gas flow). Viewed from the top (see figure 4), when travelling a distance L through the filter, the droplet will sweep out a rectangular region of area Ld_d and it will collide with any fibre that overlaps with that rectangle. The effective rectangle swept by the droplet has thus an effective area equal to $2LY$ where Y is the impact radius, *i.e.* the distance between the centre line and the line below which all the particles are captured. In the simplest case, for particles which are not deflected, we have $Y = r_d + r_f$.

(3.3) The average number of collisions N_{col} between a droplet and a fibre is thus given by the ratio between the swept area and the cross-sectional area of each fibre multiplied by the fractional area of the fibres. As the fractional area of the fibres is equal to their fractional volume $1 - \phi$, we have

$$N_{col} = (1 - \phi) \frac{2LY}{\pi r_f^2}, \quad (38)$$

and the number of collisions per unit length for a droplet is

$$\frac{N_{col}}{L} = (1 - \phi) \frac{2Y}{\pi r_f^2}. \quad (39)$$

- (3.4) As a result, the concentration of free droplets ρ_d in the filter will be described by the equation

$$\frac{d\rho_d(x)}{dx} = -(1 - \phi) \frac{2Y}{\pi r_f^2} \rho_d(x), \quad (40)$$

where x is the distance travelled through the filter. The concentration of droplets is thus

$$\rho_d(x) = \rho_d(0) e^{-\frac{x}{\lambda_p}}, \quad (41)$$

where λ_p , the average penetration length of droplets inside the filter, is

$$\lambda_p = \frac{\pi r_f^2}{2Y(1 - \phi)}. \quad (42)$$

- (3.5) If we take into account the deflection of the droplet by the gas flow, Lee and Liu [12] have shown that the effective impact radius, neglecting thermal diffusion Y_I , is given by

$$Y_I = \frac{\phi r_d^2}{(r_f + r_d)K(1 - \phi)} \quad (43)$$

where $K(1 - \phi)$ is the Kuwabara hydrodynamic function K evaluated at $1 - \phi$. The Kuwabara function is defined for arbitrary argument α by

$$K(\alpha) = -\frac{1}{2} \ln(\alpha) - \frac{3}{4} + \alpha - \frac{\alpha^2}{4}. \quad (44)$$

- (3.6) Notice that (43) was derived assuming that the droplets are smaller than the fibres, or in other words $d_f > d_d$.

- (3.7) Another factor we need to consider is the thermal diffusion of the droplets. The average distance x covered by a droplet of radius r_d in a gas of viscosity μ_G travelling through a filter at temperature T during a time t is given by

$$x^2 = 2tD_d, \quad (45)$$

where

$$D_d = \frac{k_B T}{6\pi\mu_G r_d} \quad (46)$$

and k_B is the Boltzmann constant. If we consider that the typical distance between fibres is $10\mu\text{m}$ and that the droplets move at a speed $v_d \approx 0.1\text{ms}^{-1}$, the typical time taken by a droplet to travel the distance separating the fibres is 10^{-4}s . As $k_B \approx 1.4 \times 10^{-23}\text{m}^2\text{kg s}^{-2}\text{K}^{-1}$, if we take $T = 300\text{K}$, $r_d = 0.1\mu\text{m}$ and $\mu_G = 10^{-5}\text{Pa s}$, we find $D_d = 4.5 \times 10^{-10}\text{m}^2\text{s}^{-1}$ and $x \approx 0.3\mu\text{m}$. This shows that the smallest droplets diffuse by a distance of the order of their size while they travel through the separation distance of the fibres. The net effect is to increase the capture rate and decrease the penetration length.

- (3.8) Diffusion has again been investigated by Lee and Liu [12], and they found that the effective impact radius Y_D taking into account diffusion only is

$$Y_D = 2.6r_f \left(\frac{\phi}{K(1-\phi)} \right)^{1/3} \text{Pe}^{-2/3}, \quad (47)$$

where Pe is the Peclet number defined by

$$\text{Pe} = \frac{v_G d_f}{D_d}. \quad (48)$$

- (3.9) To take into account both impact and diffusion, one simply adds the two effective impact radii Y_I and Y_D [12]:

$$Y = Y_I + Y_D. \quad (49)$$

This approximation is correct to first order.

- (3.10) In the table below we provide some values for Y_I and Y_D as well as the penetration length λ_p computed using (49). As expected, we see that for smaller droplets (of radius less than $1.5\mu\text{m}$), diffusion is the dominant factor for collision, whereas for larger droplets, diffusion becomes less important and direct collision dominates. Notice also that, for very small droplets, the diffusion is so large that the penetration length decreases with their radius. Thus the droplets that are the hardest to capture have a radius of about $0.1\mu\text{m}$.

$r_d(\mu\text{m})$	$Y_I(\mu\text{m})$	$Y_D(\mu\text{m})$	$\lambda_p(\mu\text{m})$
0.05	0.008	0.14	53
0.1	0.03	0.09	66
0.15	0.064	0.067	60
0.2	0.1	0.06	48
0.5	0.5	0.03	14
1	1.6	0.02	5

Table 2: Average penetration length and effective impact radius as a function of the droplet radius.

- (3.11) The method used by Lee and Liu [12] to evaluate the effective deflection impact radius assumes that droplets follow the flow of the gas, and neglects any inertia they might have. For this reason, the method does not work well when the droplets are larger than the fibres. Moreover, when droplets are large their diffusion is very small. In that case, one should take for the impact radius $Y = r_d + r_f$. This curve and $Y = Y_I + Y_D$, regarded as functions of r_d , intersect at $r_d \approx 1.23\mu\text{m}$, as illustrated in figure 5.

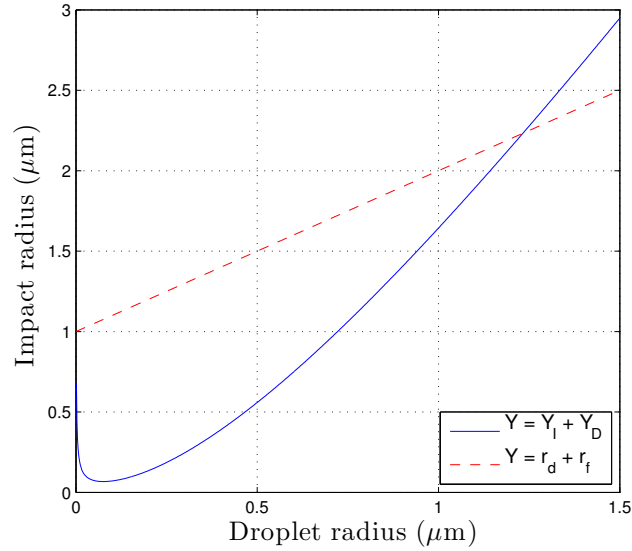


Figure 5: Impact radius Y as a function of drop radius r_d .

(3.12) On average, using (41), the number of free droplets per unit volume will be given by $n(x) = n(0)e^{-x/\lambda_p}$. Hence from table 2, even the smallest droplets, $r = 0.05\mu\text{m}$, have a very short penetration length in the dry filter, and over a distance of 0.5mm inside the filter the number of droplets is reduced by a factor of $e^{-4} \approx 0.02$. This is consistent with the data provided in [11], where the filter is split into ten segments and the largest fluid concentration is found in the segment nearest the inlet.

(3.13) By assuming that the fibres are all perfectly aligned and perpendicular to the direction of droplet flow, we have considered the optimum orientation for capture. In reality, the fibres will be randomly oriented and their effective length must be projected onto the direction perpendicular to the droplets' trajectory; then averaging must be performed over all possible orientations. The result is that the collision rate must be multiplied by a factor

$$\kappa = \frac{1}{\pi} \int_0^\pi |\sin \theta| d\theta = \frac{2}{\pi} \approx 0.64. \quad (50)$$

(3.14) The penetration length will thus be about 1.5 times greater than we have estimated in the ideal case.

(3.15) On the other hand, when the filter has reached its steady state, all the fibres will be wet and have a larger effective diameter. We then replace $1 - \phi$ by the sum of the volume fraction of the fibres and the liquid, $1 - \phi + \phi\alpha_{LM}$, and increase the effective radius of the fibres accordingly. This results in a decrease of the penetration length.

3.2 Extraction of droplets from fibre to gas

- (3.16) To study the dynamics inside the filter, we must find out how much of the fluid attached to the fibres detaches from them to become droplets again. Approximating the gas speed in the filter, u_G , by the gas speed at the inlet, the Reynolds number for the gas is

$$\text{Re} = \frac{u_G \rho_G r_f}{\mu_G} \approx 2.5, \quad (51)$$

which is effectively small (typically, $\text{Re} \approx 100$ is needed before inertia becomes important). Stokes flow considerations will therefore be applicable here.

- (3.17) We consider a droplet of radius larger than the radius of the fibre attached to it. The gas flow exerts a drag force on the droplet which can be approximated by the Stokes formula

$$F_{drag} \approx 6\pi\mu_G r_d u_G. \quad (52)$$

- (3.18) This will be balanced by the surface tension force at the contact line between the fibre and the droplet. As the hexane-Teflon contact angle is very small, the surface tension is approximately given by the hexane surface tension, and the contact line will have a length of the order of the fibre circumference. So the surface tension force is approximately

$$F_{st} \approx 2\pi\gamma_{LG} r_f. \quad (53)$$

- (3.19) For the drag force to be able to extract the droplet from the fibre we must have $F_{drag} > F_{st}$, *i.e.*

$$r_d > \frac{r_f \gamma_{LG}}{3\mu_G u_G} \approx 1\text{mm}, \quad (54)$$

where γ_{LG} is the hexane surface tension. As this far exceeds the distance between fibres, typically $10\mu\text{m}$, we can conclude that the liquid will not be extracted from the fibres, and that small captured droplets will remain attached to the fibres.

3.3 Influence of gravity

- (3.20) Another factor we would like to estimate is the importance of gravity: are droplets pulled down by gravity inside the filter or do they only flow down the side of the filter? For this, the force on the droplets due to the pressure gradient to which the liquid is subject need to be compared with the force due to gravity. For a filter of 5mm width and a pressure drop of 40kPa, we have $|\nabla p| \approx 10^7 \text{Pa/m}$, while the force per unit volume exerted by gravity is $g(\rho_L - \rho_G) \approx 4\text{kPa/m}$, where ρ_L and ρ_G are the densities of the liquid and the gas respectively. The gravitational force per unit volume acting on the fluid is thus much smaller than the pressure gradient and can be neglected.

3.4 Liquid flow rate on fibres

- (3.21) There are three distinct ways the fluid can cross the filter: it can go across as small droplets carried by the gas, it can move as large droplets attached to the fibres, or it can flow continuously along the fibres. We have already shown that liquid droplets are rapidly captured by the fibres and so we must consider the latter two transport methods. In this section, we will study the flow of fluid along the fibres. Deriving a detailed model of the fluid flow along the fibres is well beyond the scope of this report. Instead we will try to evaluate whether this method of transport can be significant by estimating the flow rate of liquid across the filter. If α_{id} denotes the inlet value of the volume fraction α_{LG} of droplets in the gas, and v_G denotes the gas face velocity at the inlet, then the volume of liquid that has penetrated a cross-sectional area S of the filter in a time t is given by

$$V_L = Sv_G\alpha_{id}t. \quad (55)$$

- (3.22) In [11] the volume fraction α_{LM} of liquid after the filter has reached steady state has been measured by splitting the filter into 10 segments between the inlet and the outlet. It was found that the volume fraction varied from 30% in the segment nearest the inlet to 15% in the segments in the middle of the filter. The volume of liquid inside the filter is given by

$$V_f = \alpha_{LM}Sl_M, \quad (56)$$

where l_M is the media/filter thickness.

- (3.23) If we assume that the liquid does not flow out until α_{LM} has reached its steady state value, the V_L and V_f are identical and we can then estimate the time needed to reach steady state to be

$$t = \frac{\alpha_{LM}l_M}{v_G\alpha_{id}}. \quad (57)$$

- (3.24) Taking $v_G = 0.1\text{m/s}$, $\alpha_{id} = 10^{-5}$, $l_M = 5\text{mm}$ and $\alpha_{LM} = 0.2$ we have $t = 1000\text{s}$, *i.e.* of the order of 15 minutes. If we take $\alpha_{id} = 10^{-6}$, then $t \approx 2.5$ hours. Notice that these estimated times also tell us how long it takes for a droplet of liquid to cross the filter. The average speed of the liquid droplet is respectively $5\mu\text{m/s}$ and $0.5\mu\text{m/s}$ for the two cases considered.

3.5 Displacement of large droplets on fibres

- (3.25) Consider a droplet during the initial stages of capture by a fibre, as shown in the schematic figure 6(a). Though depending on relative surface tension coefficients between the liquid and gas, and between the gas and solid, the droplet assumes a tapered configuration [7]. For the purpose of this study we assume a spherical droplet on the fibre. The surface energy gained due

to this wetting process is thus $E_{init} = \pi\gamma_{LG}d_f d_d$, where d_d is the droplet diameter, d_f the fibre diameter and γ_{LG} is the surface tension. For a droplet on a fibre the surface energy does not change and we assume for simplicity that the droplet translates with a velocity equal to that of the gas velocity v_g .

- (3.26) When the droplet intersects a crossing point of the fibrous network, it comes into contact with N fibres that pass through the point (see figure 6(b)). Assuming a spherical droplet once again, the surface energy gained due to adhesion with the fibres is given by $E_{node} = N\pi\gamma_{LG}d_f d_d$. Thus the net gain in energy is $\Delta E = (N - 1)\pi\gamma_{LG}d_f d_d$. This makes it possible to connect gas velocity with the droplet diameter using Stokes' formula. Thus assuming the droplet moves by one droplet diameter, and equating the work done to the change in energy ΔE , we have

$$F_{drag} \cdot d_d = 3\mu_G \pi d_d u_G \cdot d_d = (N - 1)\pi\gamma_{LG}d_f d_d, \quad (58)$$

where μ_G is the viscosity of the gas, u_G is the gas velocity, and F_{drag} is the drag force exerted on a droplet by the gas. From (58) the gas velocity is given by $u_G = (N - 1)\gamma_{LG}d_f/3\mu_G d_d$.

- (3.27) Now consider the situation when the droplet is stuck at a crossing point. The only way the droplet can move past this junction is if the work done by the force acting on it due to the gas flow is great enough to balance the interfacial energy, *i.e.* $F_{drag} \cdot d_d = \Delta E$. The drag force exerted on a droplet is given by $F_{drag} = P\pi d_d^2/4$, where P is the gas pressure and $\pi d_d^2/4$ the cross-sectional area offered by the droplet. Thus

$$P\pi d_d^3/4 = (N - 1)\pi\gamma_{LG}d_f d_d. \quad (59)$$

- (3.28) Equation (59) implies that as long as the droplet diameter is greater than the above critical value the droplet moves. Assuming a uniform accretion rate of the droplet based on the gas flow rate, this sets a time scale for droplet diameter reaching this value. The rate of change of volume of the droplet is given by

$$\frac{dV}{dt} = p_{enc} Q_v, \quad (60)$$

where Q_v is the volumetric flow rate and p_{enc} is the probability of a droplet encountering a fibrous meshwork node. Given the separation between fibres as $\ell \approx 10 - 20\mu\text{m}$ and diameters of individual fibres as $d_f \approx 2 - 5\mu\text{m}$, we estimate this probability to be approximately $p_{enc} \approx 0.2$. Since $dV/dt = 4\pi r_d^2 dr_d/dt$, where r_d is the droplet radius, equation (60) can be integrated to obtain a relation between the radius/diameter of the droplet as a function of time given by

$$d_d^3 = \left(\frac{6p_{enc} Q_v}{\pi} \right) t. \quad (61)$$

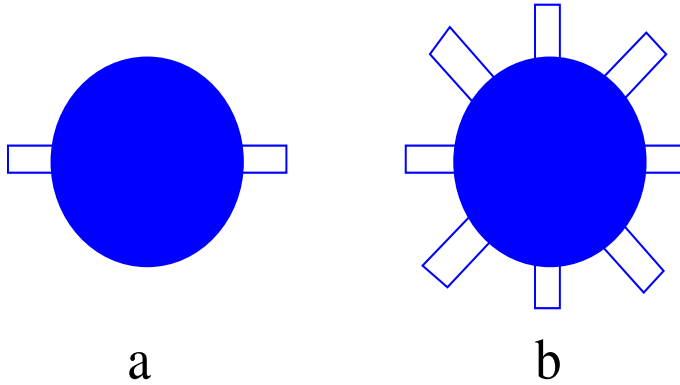


Figure 6: Schematic figure for microscopic model: (a) a single droplet wetting a fibre; and (b) a node with $n = 4$ fibres while the drop retains its spherical geometry.

(3.29) The above relation can be used to obtain estimate of the time scale over which the droplet grows past the critical threshold of equation (61), *i.e.*

$$t_{growth} = \frac{\pi d_d^3}{6p_{enc}Q_v} = \frac{\pi}{6p_{enc}Q_v} \left(\frac{4(N-1)\gamma_{LG}d_f}{P} \right)^{3/2}. \quad (62)$$

(3.30) Further assuming the mean separation between nodes $\approx \ell$, we can compute the speed of the liquid droplet to be

$$u_L = \frac{\ell}{t_{growth}} = \frac{6\ell p_{enc}Q_v}{\pi d_d^3}. \quad (63)$$

(3.31) In the regime we are analysing, the droplet undergoes stick-slip motion through the fibrous mesh akin to a particle moving over a landscape having multiple traps. Based on these ideas a Markov chain model has been developed (§4) that incorporates hopping rates of the droplets as a function of their size based on microscopic considerations. Thus for small droplets hopping from a node with N crossing points to one with $N + 1$ assuming local thermal equilibrium, the occupancies of these states are weighted by $\exp[-(E_{N+1} - E_N)/(k_B T)]$, with E_{N+1} and E_N corresponding to the respective energies, k_B being the Boltzmann constant and T the temperature. By surface energy considerations, $E_{N+1} - E_N = \pi\gamma_{LG}d_d d_f$.

(3.32) This translates to a hopping rate of the droplet as $\nu_1 \approx \nu_0 \exp[\pi\gamma_{LG}d_d d_f/(k_B T)]$ with ν_0 being an attempt frequency. For large droplets the hopping rate is set by the inverse of the timescale over which the droplet diameter grows over the critical threshold required to dislodge itself from the crossing point (59). Since $t_{growth} \sim d_d^3$, the hopping rate in this regime is given by $\nu_2 \sim \nu_0 d_d^{-3}$.

(3.33) The stick-slip model is a good model for systems where the liquid does not wet the fibre appreciably. It is also applicable for systems where the number of fibres that the droplet wets at a crossing point is not very large. Using

the parameter values provided for hexane on teflon, *i.e.* $u_G \approx v_G = 0.1\text{m/s}$, $\gamma_{LG} = \gamma_{LM} - \gamma_{GM} \approx 0.001\text{N/m}$, $d_f \approx 2\mu\text{m}$ and $\mu_G \approx 10^{-5}\text{Pa s}$, we obtain a droplet diameter of $d_d \approx 10^{-3}\text{m}$. This implies that the droplet wets $\approx (d_d/\ell) = 10^3$ fibres. In this case the assumed spherical geometry is no longer valid. A model including coalescing droplets covering several nodes has been developed.

3.6 Alternative model for droplet coalescence and translation within a filter medium

(3.34) We now consider an alternative model for how droplets coalesce and are translated through the filter medium (here assumed to be a network structure comprising nodes and connecting fibres). We note that some expressions will therefore disagree with those derived elsewhere in this chapter.

(3.35) The fundamental assumption throughout this section is that small droplets enter the filter medium and are quickly captured by fibres (small penetration depth). A droplet will translate along the capturing fibre until it reaches the nearest node. A droplet will then sit at a node, growing as it is fed with further small droplets (the coalescence phase), until a critical droplet size is reached at which the drag from the gas flow is strong enough to overcome the surface tension forces holding it at the node. In this section we estimate this critical droplet size, the time taken to attain this size, and the subsequent translation speed and transit time when large droplets begin to move through the filter matrix. This model assumes that once a large (coalesced) droplet moves off through the filter, no further coalescence occurs (steady translation speed).

(3.36) *Critical droplet size*

We need a further assumption on how the critical size for the droplet is achieved. The growing droplets sitting at nodes are fed from the influx of small monodisperse droplets arriving at the surface of the filter material via the gas flow. Since the small droplets in the aerosol are uniformly distributed, droplets will start to grow (at the same rate) at all nodes in the surface layer.

(3.37) We will show in the following that the critical droplet radius r_{dc} for being pulled off a node is larger than $l_f/2$ (one half of the inter-fibre spacing). Therefore, once the growing droplets have reached a radius of $l_f/2$, they will also touch their neighbouring droplets and very quickly coalesce into a large droplet with a critical size. We assume (perhaps arguing that a short but finite time is needed to merge into even larger droplets $r_d > r_{dc}$) that the droplets will cease growth once they reach r_{dc} , at which stage they begin to move steadily. Within our 1D framework, all moving droplets within the filter will then have the same steady speed, v_{df} , and thus no further

coalescence (or growth) will occur.

(3.38) In the following, we base our calculations and estimates on values from Kampa *et al.* [11], who carried out very careful controlled experiments on oil mist filtration. Their experimental setup is, in all important respects, very similar to the industrial rig used by Pall.

(3.39) We first show that $r_{dc} > l_f/2$ for typical experimental parameter sets. We assume that the force F acting on a droplet to drag it away from a node is due entirely to drag from the forced gas flow, and that F may be approximated by a Stokes drag. This is justified by noting that the Reynolds number for the gas based on pore size l_f is

$$\text{Re}_p = \frac{\rho_G u_G l_f}{\mu_G} \approx \frac{1 \text{ kg m}^{-3} \times 0.25 \text{ m s}^{-1} \times 4 \times 10^{-6} \text{ m}}{2 \times 10^{-5} \text{ kg m}^{-1} \text{ s}^{-1}} = 5 \times 10^{-2} \ll 1.$$

(3.40) Thus, the drag on a droplet of critical radius is

$$F = 6\pi\mu_G u_G r_{dc}.$$

(3.41) If we assume that surface tension is the dominant force holding a droplet pinned at a node, then the work done in overcoming this is approximately

$$W_{st} = 2\pi(\gamma_{GM} - \gamma_{LM})\Delta N r_f r_{dc},$$

where γ_{GM} is the surface energy (gas-solid), γ_{LM} is the interfacial energy (liquid-solid), ΔN is the difference in the number of fibres on the left and right of the droplet, and $r_f = d_f/2$ is the fibre radius (we assume that the critical droplet needs to be moved through a distance of r_{dc} in order to free it from the node). The critical radius r_{dc} is obtained by equating the work done by the Stokes drag F in moving the droplet through distance r_{dc} to W :

$$r_{dc} = \frac{(\gamma_{GM} - \gamma_{LM})\Delta N r_f}{3\mu_G u_G}. \quad (64)$$

(3.42) Taking parameter values from [11], and noting that for a wetting fluid (zero contact angle) $\gamma_{GM} \gg \gamma_{LM}$, and $\gamma_{GM} \approx \gamma_{LG} = 0.03 \text{ kg s}^{-2}$, $\Delta N = O(1)$, $r_f \approx 5 \times 10^{-7} \text{ m}$, $\mu_G = 2 \times 10^{-5} \text{ kg m}^{-1} \text{ s}^{-1}$, $u_G = 0.25 \text{ m s}^{-1}$, we find $r_{dc} \approx 2 \text{ mm}$.

(3.43) *Steady translation velocity*

Given that the critical droplet size obtained is much larger than the inter-node spacing l_f , we assume that the key forces acting on such a droplet in steady translation are the Stokes drag due to the gas, and the viscous drag imparted by the fibrous matrix. Assuming that the fibrous matrix is roughly homogeneous, then on average a droplet of given size within the

matrix will always contain the same number, N , of fibres. The value of N is related to the droplet size: larger droplets will contain more fibres. Let ϕ be the void fraction of the matrix (in practice $\phi \approx 0.95$); then $1 - \phi$ is the volume occupied by fibres. We have, for a droplet of radius r_d ,

$$1 - \phi = \frac{\text{fibre volume}}{\text{droplet volume}} = \frac{\pi l_f^2 r_d N}{\frac{4}{3}\pi r_d^3},$$

giving the number of fibres contained in a droplet of radius r_d as

$$N = \frac{4r_d^2(1 - \phi)}{3l_f^2}.$$

- (3.44) Each of these fibres imparts viscous drag to the droplet as it moves over them at speed v_{df} . We estimate the drag per fibre by

$$D_f = k_d \frac{\mu_L v_{df}}{r_d} \times 2\pi l_f r_d,$$

i.e. the droplet shear force per unit area multiplied by contact area, where k_d is a dimensionless constant of proportionality, assumed $O(1)$, giving the net drag due to all fibres as ND_f . Equating ND_f to the Stokes drag of the gas gives a relation between the droplet size r_d and its steady translation speed through the matrix, v_{df} . This relation is

$$v_{df} r_d = \frac{\mu_G u_G l_f}{k_d \mu_L (1 - \phi)}, \quad (65)$$

where μ_L is the viscosity of the liquid (hexane).

- (3.45) Equations (64) and (65) together provide an estimate for the speed of translation of a droplet of critical size, r_{dc} . Substitution of parameter values from [11] gives (apart from an order-one multiplicative constant)

$$v_{df} \sim 2.5 \times 10^{-7} \text{ m s}^{-1}. \quad (66)$$

- (3.46) For a fibrous matrix slab of thickness 5 mm, this gives a droplet transit time of order 5 hours. Since a steady state should be achieved on the order of this transit time, this estimate is in good agreement with the time of about 3.5 hours reported by Kampa *et al.* [11] to achieve steady state.

- (3.47) Kampa *et al.* [11] do not provide direct estimates for the transit speed of droplets. They do however report the level of saturation, S_0 (the percentage of void occupied by liquid locally; since the fibre fraction of the matrix is only about 5%, this is more or less the same as the percentage of total volume occupied by liquid locally). Mass conservation for the liquid gives

$$\rho_L v_{df} S_0 = I,$$

where I is the mass flux of droplets in the aerosol ($I = 0.2 \text{ kg h}^{-1} \text{ m}^{-2}$). Restricting attention to the experimental region where v_{df} is constant (i.e. the region where S_0 is constant, which is roughly the latter half of the filter slab in Kampa et al. [11]), we find

$$v_{df} \approx 6 \times 10^{-7} \text{ m s}^{-1}. \quad (67)$$

(3.48) Even though we have neglected scaling factors in deriving the theoretical value for v_{df} in (66), this value compares favourably with the estimate (67) obtained from the experimental data.

(3.49) *Residence time for initial droplet growth (coalescence)*

Denoting the volume of a node-pinned droplet by V_d , we have the residence time of a droplet at a node, T_r , given by

$$T_r = \frac{V_d - V_0}{dV_d/dt},$$

where $V_d = \pi d_d^3/6$ is the volume of a droplet with radius $r_d = d_d/2$, and V_0 is the initial volume (i.e. the volume of an incoming droplet in the aerosol). Since $V_0 \ll V_d$ we may neglect V_0 in this formula. We estimate dV_d/dt by considering the mass influx over a square region of lateral extent equal to the inter-node distance, assuming this region feeds into a single node in the interior where droplets collect. Hence

$$\frac{dV_d}{dt} = \frac{I d_d^2}{\rho_L} \approx 10^{-18} \text{ m}^3 \text{ s}^{-1},$$

and the residence time T_r during which the droplet grows but has not started to move is given by

$$T_r \approx \frac{V_d}{dV_d/dt} \approx 256 \text{ s}.$$

(3.50) This time is clearly negligible compared with the transit time it takes for a steadily translating droplet to move through the filter slab.

3.7 Fluid flow on fibres

(3.51) One possible method of fluid displacement along the fibres will be a simple flow along them. The geometry of the fibres makes it a quite complex problem, and so before embarking on a full study we can try to estimate if such a flow is likely to be realistic. For this, we assume that the fibres are all parallel to each other and parallel to the main gas flow, and that the liquid will form a cylinder around each fibre. As the hexane-Teflon contact angle is 12° , this is a reasonable, if somewhat over-simplified, assumption. We will then assume that the fluid is described by a Stokes flow on the fibres driven by the pressure gradient across the filter, and with a non-slip boundary condition on the contact region with the fibres.

(3.52) We will then consider two different boundary conditions at the contact region between the gas and the liquid. The first one will be a free boundary condition and for the second one we will impose the condition that the speed of the liquid has a fixed value, which will eventually be related to the gas speed. By solving the Stokes equation, we will be able to relate the total fluid flow to the thickness of the liquid layer on the fibres. Knowing the fibre density and the total liquid flow through the filter, we will be able to estimate the thickness of the liquid layer which, if not too large, will tell us if such a steady flow is realistic or not.

(3.53) We thus consider a fibre of radius r_f and the hollow cylinder formed by the liquid layer of outside radius R_1 such that the thickness of the liquid layer is $h = R_1 - r_f$. In cylindrical coordinates, we must then solve the equation

$$\frac{1}{r} \frac{\partial}{\partial r} \left(r \frac{\partial u_L}{\partial r} \right) = \frac{\nabla p}{\mu_L}, \quad (68)$$

where ∇p is the pressure gradient along the main axis of the fibre. To begin with, we consider the boundary conditions

$$u_L(r_f) = 0, \quad \left. \frac{\partial u_L}{\partial r} \right|_{r=R_1} = 0. \quad (69)$$

(3.54) The general solution of (68) is given by

$$u_L = \frac{\nabla p}{\mu_L} \frac{r^2}{4} + b \ln(r) + a \quad (70)$$

where a and b are two integration constants. When imposing the boundary conditions (69) we get

$$\begin{aligned} a &= \frac{\nabla p R_1^2}{2\mu_L} \ln(r_f) - \frac{\nabla p r_f^2}{4\mu_L} \\ b &= -\frac{\nabla p R_1^2}{2\mu_L}. \end{aligned} \quad (71)$$

(3.55) The total fluid flow is then given by

$$\begin{aligned} Q &= 2\pi \int_{r_f}^{R_1} r u_L dr \\ &= 2\pi \int_{r_f}^{R_1} \left(\frac{\nabla p}{4\mu_L} (r^2 - r_f^2) - \frac{R_1^2 \nabla p}{2\mu_L} \ln\left(\frac{r}{r_f}\right) \right) r dr \\ &= 2\pi \frac{\nabla p}{4\mu_L} \left[\frac{3}{4} R_1^4 + \frac{1}{4} r_f^4 - R_1^2 r_f^2 - R_1^4 \ln\left(\frac{R_1}{r_f}\right) \right]. \end{aligned} \quad (72)$$

(3.56) The pressure drop between the inlet and outlet of the filter is about $\Delta P \approx 4 \times 10^4 \text{Pa}$. As the filter has a thickness of about $l_M = 5 \text{mm}$, the pressure gradient is given by $\nabla p \approx 4 \times 10^4 \text{Pa} / 5 \times 10^{-3} \text{m} \approx 10^7 \text{Pa/m}$. The fluid flux across a filter area A is given by $Q_A = u_G A \alpha_{LG} = 10^{-7} A \text{ m/s}$. If $S_f = \pi r_f^2$ is the cross-sectional area of each fibre, the number of fibres in an area A is given by $n_A = A \times \phi / S_f \approx A \times 1.6 \times 10^{10} \text{m}^{-2}$ and the liquid flux per fibre is thus given by

$$Q_f = \frac{Q_A}{n_A} = \frac{10^{-7}}{1.6 \times 10^{10}} \frac{\text{m}^3}{\text{s}} \approx 6 \times 10^{-18} \frac{\text{m}^3}{\text{s}}. \quad (73)$$

(3.57) Equating Q_f and Q , we get an estimate for the thickness of the liquid layer on the fibres needed to sustain that liquid flux through the filter. For this we need to invert equation (72) to express R_1 as a function of Q . If we assume $R_1 = r_f(1 + \varepsilon)$, we can expand Q in powers of ε and get

$$\begin{aligned} Q &\approx 2\pi \frac{\nabla p r_f^4}{4\mu_L} \left(\frac{3}{4}(1 + \varepsilon)^4 + \frac{1}{4} - (1 + \varepsilon)^2 - (1 + \varepsilon)^4 \ln(1 + \varepsilon) \right) \\ &\approx -\frac{2\pi}{3\mu_L} \nabla p r_f^4 \varepsilon^3. \end{aligned} \quad (74)$$

As $\nabla p < 0$ with our choice of coordinates, Q is positive.

(3.58) We thus have

$$h = R_1 - r_f = \varepsilon r_f = r_f \left(|Q_f| \frac{3\mu_L}{2\pi \nabla p r_f^4} \right)^{1/3} \approx 0.2 \text{nm}. \quad (75)$$

(3.59) Hence layer of fluid required to flow on the fibres is very thin. In our evaluation we have assumed that all the fibres are optimally aligned. In reality this won't be the case, and the number of effective fibres will be smaller, but even if this is taken into account, h will remain extremely small. Notice also that our assumption that $h \ll r_f$ is indeed justified.

(3.60) For the second set of boundary conditions, we consider that the speed of the liquid at the interface with the gas has a fixed value which will be related to the average speed of the gas. This is the simplest boundary condition which we can consider and that takes the friction with the gas into account. Concretely we take

$$u_L(r_f) = 0, \quad u_L(R_1) = v, \quad (76)$$

so that

$$u_L = \frac{\nabla p}{4\mu_L} (r^2 - r_f^2) + \left(v - \frac{\nabla p}{4\mu_L} (R_1^2 - r_f^2) \right) \frac{\ln\left(\frac{r}{r_f}\right)}{\ln\left(\frac{R_1}{r_f}\right)}. \quad (77)$$

(3.61) Hence

$$\begin{aligned}
 Q &= 2\pi \int_{r_f}^{R_1} r u_L dr \\
 &= \frac{\pi}{8 \ln\left(\frac{R_1}{r_f}\right)} \left(\frac{\nabla p}{\mu_L} \left((r_f^4 - R_1^4) \ln\left(\frac{R_1}{r_f}\right) + (R_1^2 - r_f^2)^2 \right) \right. \\
 &\quad \left. + 4v \left((r_f^2 - R_1^2) + 2R_1^2 \ln\left(\frac{R_1}{r_f}\right) \right) \right). \tag{78}
 \end{aligned}$$

(3.62) If we assume that $R_1 = r_f(1 + \varepsilon)$ we have

$$Q = \pi r_f^2 \varepsilon v + O(\varepsilon^2). \tag{79}$$

(3.63) At the contact surface between the gas and the fluid we impose the condition

$$\mu_L u_L = \mu_G u_G \tag{80}$$

where μ_L , and μ_G are the dynamic viscosity of the liquid and the gas respectively. This gives

$$v = u_L \approx 0.34 \text{m/s}. \tag{81}$$

(3.64) We then have

$$h = \varepsilon r_f = r_f |Q_f| \frac{1}{\pi v r_f^2} \approx 6 \times 10^{-7} \text{nm}, \tag{82}$$

which is so small that it is outside continuum theory.

(3.65) We can thus conclude that one needs only a very small layer of liquid to generate enough flow to account for the fluid flow across the filter. This also shows that the fluid flow is more complex than we have considered here. Indeed, our simple estimates suggest that the liquid should be able to flow very easily along the fibres.

(3.66) In our description of the microscopic properties of the filter we have considered two extreme cases: the displacement of large droplets across the fibre mesh and the flow of liquid along the fibres. The real displacement must be a mix of the two. We must model the surface tension of the liquid and its flowing properties simultaneously. The pressure gradient in the gas, and the pressure induced by the gas as it flows past the liquid, will be balanced against the friction inside the liquid, the surface tension of the liquid, and the attraction forces between the liquid and the fibres. As we know, if some liquid is dropped onto a dry filter, the fibres absorb the liquid like a sponge and the liquid does not flow out of it. This sponge effect is created by the balance between the surface tension of the liquid and the attraction force between the fibres and the liquid. When the filter is active, fluid is constantly *deposited* on the inlet side of the filter, and the gas flow also induces a pressure gradient to push the liquid out of the filter, but the force that must be balanced is the attraction force exerted by the fibres on the liquid.

- (3.67) One should take into full consideration the pressure induced by surface tension of the liquid layers, the surface attraction of the liquid by the fibres, the pressure exerted by the gas at the surface of the liquid layers, and the pressure gradient in the gas. Moreover, as described elsewhere in this report, large droplets can also move across fibres and account for at least part of the fluid flow. This will require further work.

3.8 Linking the macroscopic to the microscopic model

- (3.68) *Derivation of f_d from the microscopic model*

To link the macroscopic model to the microscopic one, we must first observe that $\rho_g \alpha_g \phi = \rho_d$ and that equation (40) implies that

$$f_d = 2u_G \frac{(1 - \phi)Y}{\pi r_f^2} \rho_g \alpha_g \phi \quad (83)$$

where Y is given by

$$Y = \begin{cases} Y_I + Y_D, & r_d < 1.2 \mu\text{m} \\ r_d + r_f, & r_d > 1.2 \mu\text{m} \end{cases}$$

with Y_I and Y_D given respectively by (43) and (47).

- (3.69) *Derivation of \mathbf{F}_{LM} from the microscopic model*

The derivation of \mathbf{F}_{LM} is much more complex than for f_d . The reason is that the transport of liquid on the fibres is the result of complex microscopic phenomena. For simplicity we will assume that the liquid transport is the result of large droplets being pushed by the gas flow. Only droplets with a volume exceeding the critical volume V_c will be able to move, where

$$V_c(u_G) = \frac{4\pi}{3} \left(\frac{\Delta N \gamma_{LG} d_f}{3\mu_G u_G} \right)^3. \quad (84)$$

where ΔN is the number of fibres from which the droplet must detach itself to move and is of order 1.

- (3.70) Instead of obtaining an explicit expression for \mathbf{F}_{LM} , we re-write the equations for α_{LM} as follows:

$$\begin{aligned} \alpha_{LM} &= NV, \\ \frac{\partial \alpha_{LM}}{\partial t} + \frac{\partial (u_L \alpha_{LM})}{\partial x} &= 2u_G \frac{\phi Y}{\pi r_f^2}, \\ u_L &= \begin{cases} 0, & V < V_c \\ u_G + \frac{\partial p}{\partial x} \frac{1}{3\pi\mu_G r_d}, & V > V_c. \end{cases} \end{aligned} \quad (85)$$

- (3.71) The first equation here states that α_{LM} is expressed as a function of the droplet volume V . The second equation states that the time variation of α_{LM} is due to the displacement and capture of liquid from the gas. The last equation is obtained by integrating equation (8) and fixing \mathbf{F}_{LM} so that only the large enough droplets move.

4 Stochastic Model

4.1 Mean-field calculation of droplet size distribution in a thin coalescence filter

- (4.1) We aimed to formulate a system of equations to determine the distribution of droplet sizes among the droplets that are caught by the fibres in the filter. To do so, we first discretised the continuum of different droplet sizes in multiples of a unit droplet, corresponding to the small droplets entering the filter. Further, our basic model relies on the assumption that free droplets are all of size 1 and droplets on fibres grow only by coalescing with such free droplets passing by.

- (4.2) If we have a thin layer of fibrous material of thickness Δx , the current $j(x, t)$ of free droplets is reduced by the amount of droplets absorbed by the fibres with rate α , such that

$$\frac{j(x + \Delta x, t) - j(x, t)}{\Delta x} = \alpha \rho_f j(x, t) \quad (86)$$

where ρ_f is the density of fibres in this layer. In the case of constant ρ_f , we have $\partial_x j = \alpha \rho_f j$ and therefore $j(x, t) = j(0, t) \exp(-\alpha \rho_f x)$.

- (4.3) Now, we distinguish fibres with droplets of size $i \in \{0, \dots, n\}$ attached to them and describe the density of these fibres with $\rho_0(x, t)$ (empty fibres), $\rho_1(x, t)$ (fibres with a droplet of size 1), etc. The above equation for $j(x, t)$ then generalises to

$$\frac{\partial j(x, t)}{\partial x} = - \left(\sum_{i=0}^n \alpha_i \rho_i(x, t) \right) j(x, t). \quad (87)$$

- (4.4) We have introduced a dependence of the absorption rate on the size of the droplet on the absorbing fibre, because a droplet is more likely to coalesce with a larger droplet.

- (4.5) To simplify the problem we can now think of a very thin filter, such that the spatial dependence can be ignored. We also assume the flow j of free droplets to be constant in time. In this thin filter a density ρ_i is diminished if one of the corresponding fibres with a droplet of size i captures a droplet, and grows if a fibre with a droplet of size $i - 1$ captures a droplet. Both

events also depend on the amount of free droplets given by the flow j . In addition, the droplets of maximal size are able to detach and leave the filter with rate b . The dynamics of these densities can be described by a system of equations of the form

$$\partial_t \rho_0 = -j\alpha_0 \rho_0 + b\rho_n \quad (88)$$

$$\partial_t \rho_i = j(\alpha_{i-1} \rho_{i-1} - \alpha_i \rho_i) \quad \text{for } i \in \{1, \dots, n-1\} \quad (89)$$

$$\partial_t \rho_n = j\alpha_{n-1} \rho_{n-1} - b\rho_n. \quad (90)$$

(4.6) This system of equations can be easily solved in the steady state, $\partial_t \rho_i = 0$. Using that the density of all fibres is constant, $\sum_{i=0}^n \rho_i = 1$, we get

$$\rho_n = \left(1 + \frac{b}{j} \left(\sum_{i=0}^{n-1} \frac{1}{\alpha_i} \right) \right)^{-1}, \quad (91)$$

$$\rho_i = \frac{1}{\alpha_i} \frac{b}{j} \rho_n \quad \text{for } i \in \{0, \dots, n-1\}. \quad (92)$$

(4.7) For this simplified system we can explore the parameter space, in particular varying the ratio j/b and size-dependence of the absorption rate α_i . Since j^{-1} is the time scale of absorption of droplets, and b^{-1} is the time scale of detachment of droplets at the largest scale, the ratio j/b describes the retention of the largest droplets, i.e. if j/b is large then the filter absorbs material faster than it loses large droplets and ρ_n will be large compared to densities of other droplet sizes, and conversely if j/b is small then ρ_n will be small, as can be seen from (91) (figure 7).

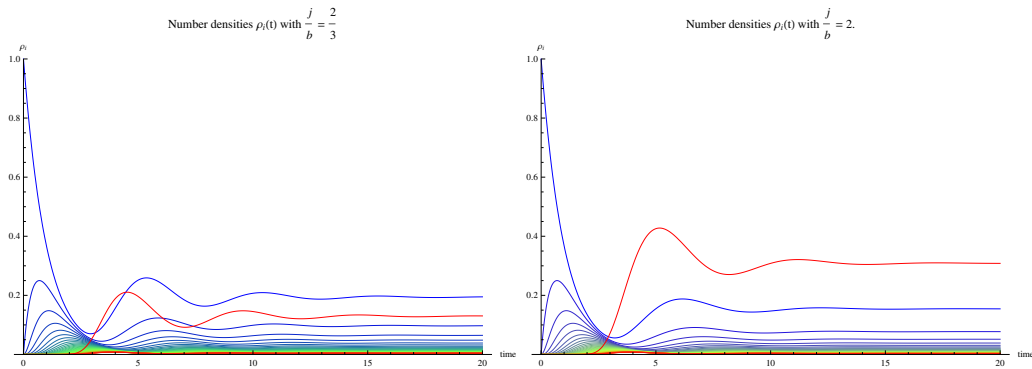


Figure 7: Time evolution of number densities for different values of j/b . If the current of free droplets is larger with respect to b , then fibres with largest droplets will dominate (red line). Number of sizes is $n = 50$, colour denotes sizes from blue (empty fibre) to red (fibre with maximum droplet size), and α scales linearly in droplet size.

(4.8) The time evolution of the system depends on the scaling of the absorption rates with droplet size, as can be seen, for example, from figure 8 in which case there is a transient oscillation when α is proportional to the size to the power $2/3$, which is not present when this power is 2.

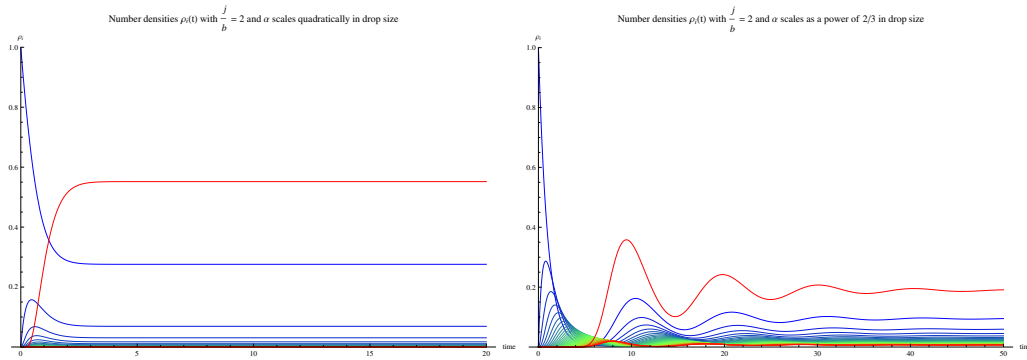


Figure 8: Time evolution of number densities for different scalings of α with droplet size. Number of sizes is $n = 50$, and colour denotes sizes from blue (empty fibre) to red (fibre with maximum droplet size).

4.2 Markov model

(4.9) We consider a continuous time Markov process to model coalescing particles travelling through a network. The particles in the model coalesce if they occupy the same node in the network, and the rate at which particles jump depends only on the size of the particle. These rates depend on the fluid dynamics at a microscopic level. There also exists an influx of particles into the system.

(4.10) We consider a second level of detail, crossing points and non-crossing points in the fibre structure. If a particle is on a fibre crossing, particles jump as discussed above, and if a particle is not on a fibre crossing, we assume it moves at the same rate as the incoming particles. The rate function (according to the fluids) is defined as

$$r(k) = \begin{cases} e^k & k < k_c \\ k^{-3} & k > k_c. \end{cases} \quad (93)$$

(4.11) The parameters for this model are the cross-over between regimes is the jump rates, k_c , and the incoming rate of particles u . Here we are also assuming all crossing points in the fibre are identical.

(4.12) We predict this model to show different phases as we vary the influx of particles and vary the cross-over regime in the jump rate function. This phase change will be a non-saturation/saturation transition. We define saturation to be a phase where we have at least one site where the number of particles is of the order of the total number of particles in the system.

(4.13) *The mathematical model*

Consider a one dimensional chain labelled $\lambda_L = \{1, 2, 3, \dots, L\}$ and configurations $\eta \in \mathbb{N}^{\lambda_L}$. Thus η is a vector encoding the number of particles at

each point in the lattice. At site 1, particles enter the system at rate u , and at site L , particles leave the system.

(4.14) *The generator*

The generator for a Markov process corresponds to the rate of change of the expected value of an observable. For example, the generator for the total number of particles, or maximum occupancy, corresponds to

$$\frac{d}{dt}\mathbb{E}f(X_t) = \mathbb{E}\mathcal{L}f(X_t). \quad (94)$$

(4.15) For an observable $f : \mathbb{N}^{\lambda L} \rightarrow \mathcal{R}$,

$$\begin{aligned} \mathcal{L}f(\eta) = & \sum_{x|x \in \{\text{crossover}\}} r(\eta_x)(f(\eta + \eta_x(\delta_{x+1} - \delta_x)) - f(\eta)) \\ & + \sum_{x|x \in \{\text{non-crossover}\}} u(f(\eta + \eta_x(\delta_{x+1} - \delta_x)) - f(\eta)) \\ & + u(f(\eta + \delta_1) - f(\eta)). \end{aligned}$$

(4.16) The first term corresponds to particles moving on fibre crossings, the second term to particles detaching from the fibres, and the third term to the incoming particles. If we take our observable to be the indicator function, $f(\eta) = \mathbb{I}_\xi(\eta)$, we find the master equation for a continuous time Markov process.

(4.17) *Average number of particles*

Consider the observable $f(\eta) = \sum_x \eta_x = N(t)$. To calculate the rate of change of the average number of particles we apply the generator to $N(t)$ and take expectations; we find

$$\frac{d}{dt}\mathbb{E}(N(t)) = \mathbb{E}(\mathcal{L}(N(t))) = u - \mathbb{E}(\eta_L r(\eta_L)). \quad (95)$$

(4.18) Therefore to see an approximately constant number of particles in the system we need the relation

$$u \approx \mathbb{E}(\eta_L r(\eta_L)), \quad (96)$$

i.e. the incoming rate of particles must balance the expected value at the final lattice site multiplied by the rate at which particles leave that site.

(4.19) *Understanding saturation*

We can consider a saturation effect occurring when there exists a lattice site such that the number of particles on that site is of the same order as the total number of particles in the system. That is,

$$\eta_{max} = \max_x(\eta_x). \quad (97)$$

(4.20) Once again we can apply the generator and calculate how the expectation of η_{max} changes in time.

(4.21) *The current through the system*

The current (across a bond in the network) is defined as the average number of jumps per unit time and will depend on the density of the system. We call this $j(\rho)$ where ρ is the density. Thus

$$j(\rho) = u + \mathbb{E}(\eta_x r(\eta_x)). \quad (98)$$

(4.22) *Simulating the Markov process*

To simulate the Markov process we use the random sequential update algorithm. We first initialise the configuration vector to the zero vector, or we randomly distribute particles onto the lattice. We also create the fibre structure by randomly distributing crossing points with a probability that gives us the correct void fraction. The total rate of the system is given by $R(t) = \sum_x r(\eta_x(t)) + u$ and the time to the next event, or waiting time, $W(t)$, is an exponentially distributed random variable $W(t) \sim \exp(R(t))$. The particle at site x jumps with probability

$$\frac{r(\eta_x(t))}{R(t)}$$

and a particle is added, due to the influx, with probability

$$\frac{u}{R(t)}.$$

(4.23) *Future work*

Higher levels of complexity can be easily incorporated into this model. One way is to increase the number of dimensions and include gravity. Currently the model only incorporates particles moving on a homogeneous fibre structure; however, the rate at which a particle moves not only depends on the size of the particle but also on how many crossings are present.

5 Lattice-Boltzmann Computation

(5.1) *Modelling the gas flow using an LBM Code*

Given the geometry of the filter setup, it is fairly straightforward to implement a Lattice-Boltzmann simulation. The basic idea behind this method is to keep discretized information on a fictional ensemble of particles. At each spatial discretization point, the occupation number of particles with a discrete set of velocities (pointing, usually, to the neighboring cells) is advected at the respective velocities. In a second step, an equilibrium distribution of velocities is calculated from the occupation numbers, and the velocities are relaxed towards this equilibrium (Maxwellian) distribution with a mixing

time constant. Boundary conditions are easy to implement, and in particular, hard reflective boundary conditions simply lead to a reflection of the velocity occupation numbers. Using such a Lattice-Boltzmann code, it is possible to accurately simulate the gas flow through the filter and the surrounding pipe.

- (5.2) *Advecting the vapour and the liquid phase*
(N.B. “Vapour” here refers to the liquid droplets in the gas flow.)

- (5.3) The output of the Lattice-Boltzmann simulation consists of an average velocity and gas density for each discretization cell. This information can be used to advect a vapour flow using, for example, a simple upwinding scheme with appropriate boundary conditions. In addition, the vapour equation should include a decay term to model the capture of vapour by the filter fibres. A possible equation to model this is

$$\frac{\partial}{\partial t}\rho_V = \mathbf{u} \cdot \nabla \rho_V - \alpha \|\mathbf{u}\| \chi_{\text{Filter}} \rho_V,$$

where \mathbf{u} is the gas velocity, ρ_V is the vapour density, χ_{Filter} is the characteristic function of the filter material, and α is a decay constant.

- (5.4) The vapour captured by the filter should be added to a liquid phase, also possibly modelled by an advection equation. In this case, to implement the stick-slip behavior of the liquid droplets, it is reasonable to advect them using a mobility and a force consisting of the gas velocity and gravity. This results in a model of the type

$$\frac{\partial}{\partial t}\rho_L = M(\rho_L)(\mathbf{u} - g\mathbf{e}_2) \cdot \nabla \rho_L + \alpha \|\mathbf{u}\| \chi_{\text{Filter}} \rho_V,$$

where ρ_L is the liquid density, $M(\rho_L)$ denotes the mobility (for example zero up to a critical value of ρ_L , and unity thereafter), and $-g\mathbf{e}_2$ denotes the gravity vector.

- (5.5) Both the equation for ρ_V and ρ_L require appropriate boundary conditions. One possibility is a zero Dirichlet boundary condition on the domain and filter boundary, respectively.

- (5.6) *Coupling of the gas flow to the liquid phase*

One interesting aspect of such an implementation is that it is very easy to include a coupling of the liquid phase back to the gas flow. This can be achieved by including an additional scattering term, where a fraction of the velocities (depending on the liquid density) gets reflected inside the filter.

A Appendix: Notation for the continuum model

Notation	Meaning
A	Dimensionless parameter used in the simplified 1D model
B	Dimensionless parameter used in the simplified 1D model
D_d	Thermal diffusion coefficient of droplets in the gas flow
D_f	Viscous drag force on a droplet imparted by a fibre
E	Dimensionless parameter used in the simplified 2D model
E_{init}	Surface energy gained due to wetting a fibre
E_{node}	Surface energy gained by wetting a fibre network node
F	The force required to drag a droplet away from a node
F_{drag}	Stokes drag force on a droplet attached to the fibres
F_{st}	Surface tension force on a droplet attached to the fibres
\mathbf{F}_{LM}	Frictional force per total volume acting on the liquid attached to the fibres
H	Column height
I	Mass flux of droplets in the aerosol
K	The Kuwabara hydrodynamic function
L	Distance travelled through the filter
N	Number of fibres
N_{col}	Average number of collisions between a droplet and a fibre
P_0	Inlet gas pressure
Pe	Peclet number for droplets in the gas flow
Q	Total fluid flow
Q_A	Fluid flux across a filter area A
Q_f	Liquid flux per fibre
Q_v	Volumetric flow rate
R_1	Outer radius of the hollow cylinder formed by liquid attached to fibres
Re	Reynolds number for the gas based on filter width
Re_p	Reynolds number for the gas based on pore size
S	A cross-sectional area of the filter
S_0	Saturation level
S_f	Cross-sectional area of a fibre
T	Temperature inside the filter
T_r	Residence time of a droplet at a node
V	Drop volume
V_0	Volume of an incoming droplet in the aerosol
V_L	Volume of liquid that has penetrated the filter
V_c	Critical drop volume required to move
V_d	Volume of a node-pinned droplet
V_f	Volume of liquid inside the filter

Table 3: Notation relating to the continuum model: I.

Notation	Meaning
W	Filter width
W_{st}	Work done to overcome surface tension at a node
Y	Impact radius
Y_D	Impact radius based on thermal diffusion only
Y_I	Impact radius based on direct collision only
d_d	Droplet diameter
d_f	Fibre diameter
f_d	Deposition rate
\mathbf{g}	Acceleration due to gravity
g	Magnitude of \mathbf{g}
h	Thickness of the liquid layer on fibres
k_d	Proportionality constant in the expression for D_f
k_G	Permeability of the filter by the gas
k_{LM}	Permeability of the filter by the liquid attached to the fibres
k_{LM0}	A reference value for k_{LM}
l	Mean separation between fibre nodes
l_f	Fibre separation distance
l_M	Media thickness
n	Number of free droplets
n_A	Number of fibres in a filter area A
p	Pressure field
p_{enc}	Probability that a drop encounters a fibre node
r	Radial coordinate in a coordinate frame based on a fibre
r_d	Droplet radius
r_{dc}	Critical droplet radius for being pulled off a node
r_f	Fibre radius
t	Time
t_{growth}	Time scale over which the drop grows past the critical size threshold
x	Horizontal spatial coordinate
y	Vertical spatial coordinate
\mathbf{u}_G	Velocity field of the gas
\mathbf{u}_L	Velocity field of the liquid
u_G	Gas speed (1D)
u_L	Speed of liquid on fibres (1D)
v	Radial speed of the liquid at the liquid-gas interface
v_G	Gas face velocity
v_{df}	Steady droplet speed assumed in §3.6
ΔE	Net gain in energy when a drop reaches a fibre node
ΔN	Difference between number of fibres at the left and right of a node
ΔP	Pressure drop across filter

Table 4: Notation relating to the continuum model: II.

Notation	Meaning
α_G	Fluid volume fraction of gas
α_{LG}	Fluid volume fraction of liquid in the gas flow
α_{LG0}	A reference value for α_{LG}
α_{LM}	Fluid volume fraction of liquid attached to fibres
α_{LM0}	A reference value for α_{LM}
α_{id}	Volume fraction of liquid in the inlet gas stream
β	Constant of proportionality used in the simplified continuum models
ε	Ratio of filter width to filter height
γ_{GM}	Surface tension between the gas and fibres
γ_{LG}	Surface tension between the liquid and gas
γ_{LM}	Surface tension between the liquid and fibres
κ	Pre-factor for the collision rate
λ_{LM}	Microscopic variables relevant to the macroscopic model
λ_p	Average penetration length of droplets insider the filter
μ_G	Viscosity of the gas
μ_L	Viscosity of the liquid attached to the fibres
ν_0	Reference value for the hopping rate
ν_1	Hopping rate based on surface energy considerations
ν_2	Hopping rate for large droplets
ρ_G	Density of the gas
ρ_L	Density of the liquid
ρ_d	Concentration of free droplets
ϕ	Void fraction of the filter

Table 5: Notation relating to the continuum model: III.

Bibliography

- [1] S. Andan, *Modeling of drainage in coalescence filtration*, PhD Thesis, University of Akron (2010).
- [2] J. F. Bitten, *Coalescence of water droplets on single fibers*. Journal of Colloid and Interface Science **33**, 265–271 (1970).
- [3] H. Cheng & G. Papanicolaou, *Flow past periodic arrays of spheres at low Reynolds number*. Journal of Fluid Mechanics **335**, 189–212 (1997).
- [4] R. V. Craster & O. K. Matar, *On viscous beads flowing down a vertical fibre*. Journal of Fluid Mechanics **553**, 85–105 (2006).
- [5] S. Dawar & G. G. Chase, *Drag correlation for axial motion of drops on fibers*. Separation and Purification Technology **60**, 6–13 (2008).
- [6] S. Dawar & G. G. Chase, *Correlations for transverse motion of liquid drops on fibers*. Separation and Purification Technology **72**, 282–287 (2010).

- [7] P. G. de Gennes, F. Brochard-Wyart & D. Quéré, *Capillarity and Wetting Phenomena: Drops, Bubbles, Pearls, Waves*. Springer, New York (2002).
- [8] C. Duprat, C. Ruyer-Quil & F. Giorgiutti-Dauphiné, *Spatial evolution of a film flowing down a fiber*. *Physics of Fluids* **21**, 042109, 1–16 (2009).
- [9] T. Frising, D. Thomas, D. Bémer & P. Contal, *Clogging of fibrous filters by liquid aerosol particles: experimental and phenomenological modelling study*. *Chemical Engineering Science* **60**, 2751–2762 (2005).
- [10] S. A. Hosseini & H. V. Tafreshi, *Modeling particle-loaded single fiber efficiency and fibre drag using ANSYS-Fluent CFD code*. *Computers & Fluids* **66**, 157–166 (2012).
- [11] D. Kampa, S. Wurster, J. Buzengeiger, J. Meyer & G. Kasper, *Pressure drop and liquid transport through coalescence filter media used for oil mist filtration*. *International Journal of Multiphase Flow* **58**, 313–324 (2014).
- [12] K. W. Lee & B. Y. H. Liu, *Theoretical study of aerosol filtration by fibrous filters*. *Aerosol Science and Technology* **1**, 147-161 (1982).
- [13] R. Mead-Hunter, A. J. C. King, G. Kasper & B. J. Mullins, *Computational fluid dynamics (CFD) simulation of liquid aerosol coalescing filters*. *Journal of Aerosol Science* **61**, 36–49 (2013).
- [14] J. I. Rosenfeld & D. T. Wasan, *Coalescence of drops in a liquid-liquid dispersion by passage through a fibrous bed*. *The Canadian Journal of Chemical Engineering* **52**, 3–10 (1974).
- [15] A. L. Yarin, G. G. Chase, W. Liu, S. V. Doiphode & D. H. Reneker, *Liquid drop growth on a fiber*. *AIChE Journal* **52**, 217–227 (2006).